

# Operation of an X-ray Undulator in the Tristan Main Ring as a Prototype of Future Super Light Sources

Shigeru Yamamoto, Hiroshi Sugiyama, Kimichika Tsuchiya and Tatsuro Shioya

Photon Factory, National Laboratory for High Energy Physics, Oho, Tsukuba, Ibaraki 305, Japan. E-mail: shigeru@kekvox.kek.jp

(Received 30 October 1996; accepted 20 December 1996)

A 5.4 m-long 239-pole undulator comprising three rigid and precise standardized-unit undulators was completed and installed in the Tristan main ring, which was operated as a light source at a beam energy from 8 to 10 GeV. This undulator was successfully tested, characterized and used as a brilliant hard X-ray source for several synchrotron radiation experiments during the last 3.5 months of 1995.

**Keywords:** undulators; insertion devices; hard X-ray sources; large accelerators as light sources.

## 1. Introduction

Since 1991, we have strongly pursued the possibility of a complete conversion of the high-energy accelerator, the Tristan main ring (MR) of the National Laboratory for High Energy Physics, KEK, Tsukuba, Japan, to a brilliant synchrotron radiation source, which is to be called the 'Tristan Super Light Facility' (TSLF). In this project the TSLF was characterized by a very low electron-beam emittance of the order of 1 nm rad, by 70 m-long undulators for hard X-rays, and by free-electron lasers for soft X-rays, as reported in the *Tristan Super Light Facility; Conceptual Design Report 1992* (1993). Since the total length of the undulators required for the TSLF amounts to more than 400 m, it is not practical to construct such undulators based on a device-by-device policy from the viewpoints of both the design and the construction costs as well as from that of manpower for commissioning and operation. In order to avoid this situation we carried out research and development studies by constructing a 5.4 m-long prototype undulator (Yamamoto, 1995; Yamamoto, Shioya, Kitamura & Tsuchiya, 1995) in which (i) three unit undulators are used to form the prototype, and (ii) for long undulators of ~70 m length the mechanical frames used for this prototype will be reproduced and connected longitudinally.

Although our original plan for the TSLF was not approved, we were finally able to carry out feasibility studies in the autumn of 1995 using very brilliant synchrotron radiation from the above-mentioned prototype undulator (named XU#MR0), which was installed in the MR. In order to create free space for installing the XU#MR0, two normal bending magnets at the end of the arc section of the MR were replaced by two short bending magnets. The modification of the MR lattice (Kamada, 1997) for this purpose was not complete compared with the original TSLF, but enabled us to reach a very low value of the natural-beam emittance of 5 nm rad (and 2% of

**Table 1**  
Parameters of the XU#MR0.

Magnetic structure	Pure configuration
Magnetic material	NdFeB ( $B_r = 12.8$ kG, $iH_c = 17$ kOe)
Period length, $\lambda_u$	4.5 cm
Number of periods	120 (= $3 \times 40$ per unit undulator)
Magnet length	5.4 m (= $3 \times 1.8$ m per unit undulator)
Maximum peak field, $B$	2.64 kG
Maximum $K$	1.11
Range of magnet gap	3–50 cm
Aperture	2.4 cm

emittance coupling) at 10 GeV and 10 mA operation of the MR as a design value. A 100 m light beamline (Sugiyama, Zhang, Higashi, Arakawa & Ando, 1997) was placed along the long straight section of the MR and synchrotron light was introduced into an experimental station located in a large experimental hall, which was formerly used for high-energy physics experiments.

In the present paper we describe the commissioning of the XU#MR0, which includes its modification required for installation into the above-mentioned MR lattice. Further, we report on a spectrum measurement of brilliant synchrotron radiation from the XU#MR0.

## 2. Installation and commissioning of the XU#MR0

The XU#MR0 (Table 1) comprises three precise standardized-unit undulators (Yamamoto, 1995; Yamamoto *et al.*, 1995). Each standardized unit (1.8 m long) is placed very precisely on a rigid common frame to form a 5.4 m undulator. We adopted a pure Halbach-type configuration of NdFeB magnets (remanent field,  $B_r = 12.8$  kG; coercivity,  $iH_c = 17$  kOe). The selection of the period ( $\lambda_u = 4.5$  cm) was made so that the Mössbauer energy of  $^{57}\text{Fe}$  (= 14.4 keV) could be obtained at the first harmonic at 10 GeV operation of the MR. The support

structure of the XU#MR0 is shaped like the letter 'C' so that it can be installed without breaking the vacuum of the MR.

The spectrum corresponding to this case (beam energy,  $E = 10$  GeV; beam current,  $I = 10$  mA; natural emittance,  $\varepsilon_0 = 5$  nm rad; emittance coupling,  $\kappa = 2\%$ ) is shown in Fig. 1. Calculations show that the XU#MR0 is able to produce quasi-monochromatic X-rays as the first harmonic with a brilliance of  $3.0 \times 10^{18}$  photons  $s^{-1} \text{mm}^{-2} \text{mrad}^{-2}$  (0.1% bandwidth) $^{-1}$  in the case of  $K = 0.97$  at 14.4 keV, when the MR is operated at 10 GeV and 10 mA with the above beam quality. By combining 8 and 10 GeV operation, photon energies from 8.4 to 21 keV can be covered by the first harmonic, and those from 25 to 60 keV can be covered by the third harmonic.

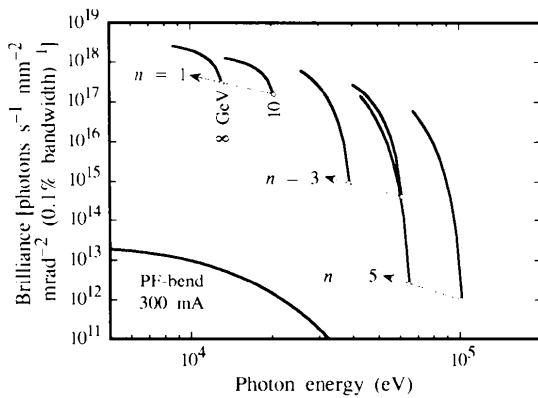


**Figure 1**

Brilliance of radiation from the XU#MR0 in the cases of 8 and 10 GeV operation of the MR with a beam current of 10 mA. Each curve shows the locus of the peak position of the  $n$ th harmonic when  $K$  decreases from its maximum. The brilliance of the radiation from the Photon Factory bending magnets at 300 mA operation is also shown for comparison.

In addition to the precise field adjustment of the XU#MR0 (Yamamoto, 1995; Yamamoto *et al.*, 1995), long coils are installed for an *in-situ* field correction in both the horizontal and vertical directions. The correction in the vertical field can be made by a pair of coils wound around the upper and lower magnet arrays of the XU#MR0. The horizontal correction can be made by a single coil wound on the vacuum chamber of the XU#MR0 along the electron beam axis. This coil was attached to the inner side of the MR with respect to the beam axis since there was no room for the horizontal correction coil on the outer side part of the chamber.

For third-generation light sources, the natural emittance of the electron beams becomes very small (a typical value is 5 nm rad, as in the present case), and in the vertical direction the condition of the diffraction limit is almost achieved. Even if the field adjustment of the undulator is completely made to match the condition of the diffraction limit before its installation, the brilliance and coherence properties of the radiation would deteriorate if the ambient magnetic field in the accelerator changes from that when the field adjustment was made. In the present case, the permitted value of the field error in terms of the kick angle of the undulator orbit is  $5 \mu\text{rad}$ , which corresponds to a change in the ambient field of as little as 0.3 G if it occurs uniformly in the total length of the undulator. Therefore, the use of these long coils is very important when they are combined with an observation of the radiation.

In order to install the XU#MR0 into the MR for test experiments, some modification of the common frame of the XU#MR0 was required, since the beam-path height of the installation point (located at the arc section of the MR) available in the present conversion of the MR is shorter by 600 mm than that (located at the long straight section) planned in an original TSLF. In order to resolve this problem, we reconstructed the common frame of the

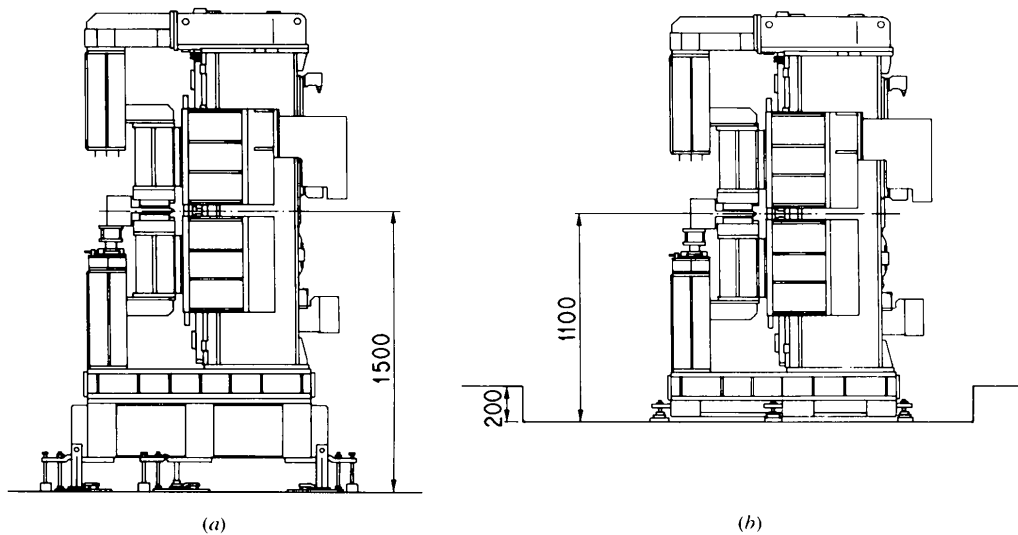


**Figure 2**

Installation of the XU#MR0 and difference in the floor level in the MR tunnel: (a) installation at the long straight section; (b) installation at the arc section.

XU#MR0 to a slim version with a height of 100 mm (the original had a height of 500 mm), and also lowered the floor level of the installation point by making a pit 200 mm deep (Fig. 2). The effects of reassembling the entire system of the XU#MR0 using this new common frame (for a magnetic field of the XU#MR0) are negligibly small if the reconnection of each unit undulator is made carefully with an accuracy of  $\pm 10 \mu\text{m}$ .

The arrangement of the XU#MR0 and magnets adjacent to it is shown in Fig. 3. In the present case the XU#MR0 was placed between the short bending magnets (SB1 and SB2 in Fig. 3), which were newly fabricated and placed so as to create a free space for installing the XU#MR0. Fig. 4 shows photographs of the XU#MR0 after the installation. For aligning the undulator and beamline system we adopted the following procedure: (i) the undulator XU#MR0 was aligned using the nearest quadrupole magnets (QSF2 and QRF4 in Fig. 3) by taking the bending angle due to SB1 and SB2 into account; (ii) the beamline was independently aligned using the quadrupole magnets in the long straight section of the MR as targets, where the relationship between the beamline and the long straight quadrupole magnets was determined on the basis of the designed value of the bending angle between the undulator axis and the long straight section. However, we found that the undulator axis was inclined by as much as 0.5 mrad in the horizontal plane with respect to the beamline axis, and that this was due to a misalignment between the arc and the long straight sections in the MR. Fortunately, in this case, since the beamline was the only one in the MR, we realigned the XU#MR0 directly along the beamline in turn, and decided that the bending angle should be adjusted during the operation of the MR.

### 3. Operation and characterization of the undulator radiation

Operation of the MR for the test experiment was started on 18 September 1995 and the electron beam was stored as

early as 20 September 1995. X-rays from the XU#MR0 were successfully introduced to the beamline by using light-axis monitors made of graphite wires (Shiwaku & Zhang, 1997); horizontal and vertical positions of the light axis were detected by these monitors which were placed at points 17, 49 and 84 m from the centre of the XU#MR0. The XU#MR0 provided X-rays very stably for commissioning the double-crystal monochromator and for the various types of utilization until the end of the test experiments on 27 December 1995 (see *e.g. Photon Factory Activity Report '95, 1996*).

Beam tuning, *i.e.* optimization of the operation parameters of the MR, was performed during 8 and 10 GeV operation of the MR where the synchrotron radiation experiments were carried out; the beam was first tuned at 8 GeV, since the injection energy was 8 GeV, and followed by synchrotron radiation experiments at 8 GeV. The beam tuning was repeated at 10 GeV before experiments at 10 GeV. This process caused a dilemma between the best-tuned operation of the MR for synchrotron radiation experiments and the longest time allocation for experiments under the condition of a strictly limited time allowed for the MR for synchrotron radiation operation (some 3.5 months). In order to carry out this process very quickly and efficiently, the vertical divergence ( $\Sigma_{y'}$ ) of the X-rays from the XU#MR0 was used as a measure of the status of the electron-beam quality after conversion to electron-beam divergence ( $\sigma_{y'}$ ) by a proper deconvolution, which took into account the effects from the divergence of the X-rays themselves and those from the optical elements used. The measurement of  $\Sigma_{y'}$  was made by taking rocking curves of the Si 400 analyzer placed after the Si 400 double-crystal monochromator, the first crystal piece of which was cryogenically cooled by liquid nitrogen. Details concerning this measurement will be given elsewhere (Sugiyama *et al.*, 1997).

During the beam tuning process at 8 GeV we found that  $\sigma_{y'}$  amounted to some 20  $\mu\text{rad}$ , which was four times larger

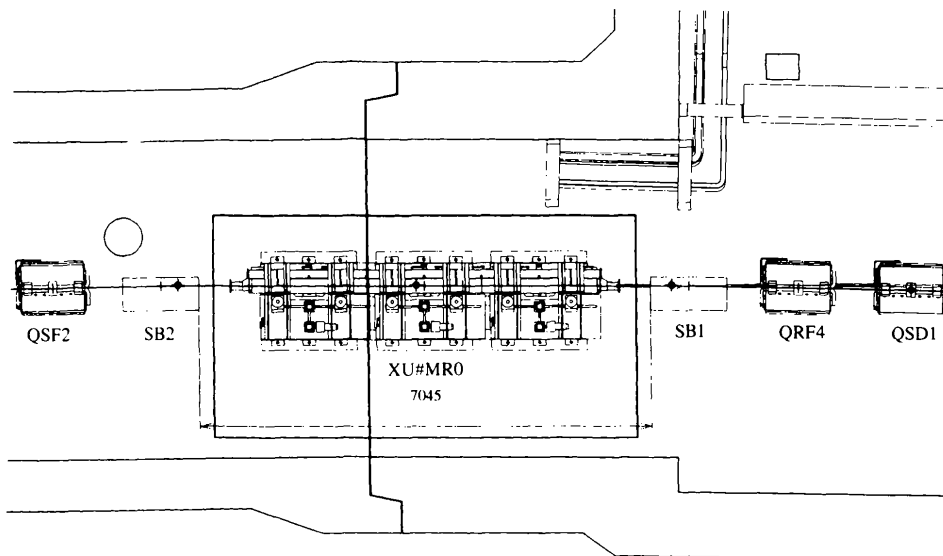
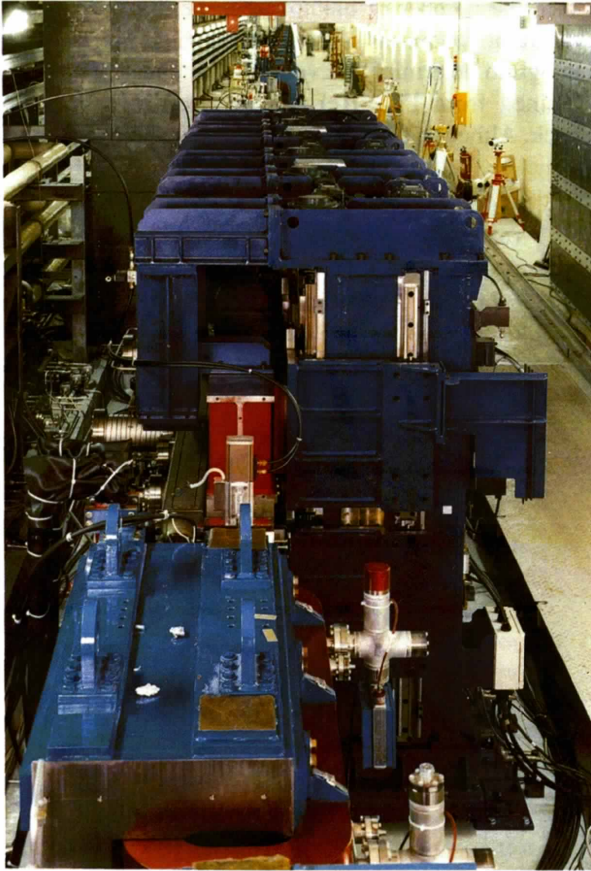


**Figure 3**  
Arrangement of the XU#MR0 and the adjacent magnets in the MR.

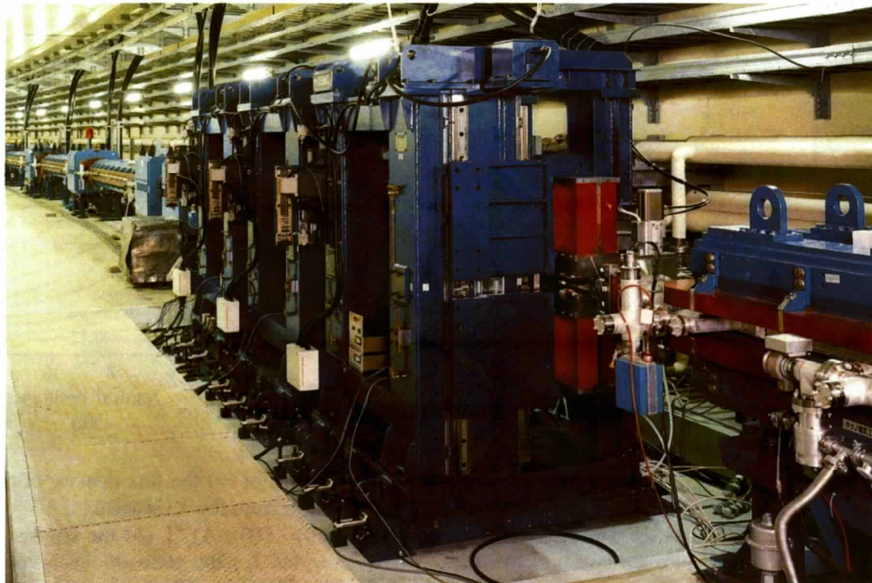
than the design value ( $4.5 \mu\text{rad}$  when  $\varepsilon_0 = 5 \text{ nm rad}$  and  $\kappa = 2\%$  is achieved). After an intensive search of the operation parameters of the MR, including a reduction of the beam current dependence of  $\sigma_{y'}$ , made by the Tristan accelerator group, the beam quality was optimized and a  $\sigma_{y'}$  value of

$8.5 \mu\text{rad}$  was obtained. Further, in this process we found that  $\sigma_{y'}$  was optimized by the long coil for the horizontal field correction (Sugiyama *et al.*, 1997). A minimum value of  $\sigma_{y'}$  ( $= 7 \mu\text{rad}$ ) was obtained at a coil current of  $-8$  to  $-10 \text{ A}$ . This phenomenon suggests that the changes in the ambient magnetic field occurred around the XU#MR0 in the MR under operation, and that these long coils are very useful for correcting this kind of change in the ambient field. A similar optimization of  $\sigma_{y'}$  was also observed at  $10 \text{ GeV}$  operation of the MR;  $\sigma_{y'} = 7.6 \mu\text{rad}$  without correction was optimized to  $\sigma_{y'} = 6.6 \mu\text{rad}$  at the correction current of  $-8 \text{ A}$ . This correction was kept constant during the synchrotron radiation experiments at  $10 \text{ GeV}$ .

A spectrum measurement as a characterization of the light source was finally performed at  $10 \text{ GeV}$  during the last three days of synchrotron radiation experiments with the MR. Instead of measuring the brilliance, we measured the on-axis photon flux density using the present optical system (Fig. 5). Radiation from the XU#MR0 was introduced to a PIN photodiode detector through an absorber made of aluminium and an  $xy$  slit (with an aperture of  $0.2 \times 0.2 \text{ mm}^2$ ), which were placed after the Si 400 double-crystal monochromator. We used a PIN photodiode which was precisely calibrated (Ban *et al.*, 1994) in a photon energy region from  $7$  to  $40 \text{ keV}$ , whereas we used a combination of an NaI scintillation counter and photons having 'fixed' energy from  $^{57}\text{Fe}$  Mössbauer nuclei in our previous study on the spectrum from the in-vacuum-type X-ray undulator installed in the Tristan Accumulation Ring, KEK, Tsukuba, Japan (Yamamoto *et al.*, 1993). An Al absorber was used for separating the first and the second harmonics of the radiation from higher harmonics. The effects of absorption, which were caused from the graphite and beryllium windows, and air in the beam path, and those of reflection efficiencies and bandwidths of the monochromator were



(a)



(b)

**Figure 4**

Photographs of the XU#MR0 after installation: (a) view from upstream along the photon beam axis; (b) view from inside the MR.

also taken into account for a correct estimation of the photon numbers (Sugiyama *et al.*, 1997).

The measured spectrum is shown in Fig. 6 as solid circles. The parameters of the light source were:  $E = 10$  GeV,  $I = 10$  mA (normalized) and  $K = 1.09$  (the first harmonic energy of 13.1 keV). Fig. 6 also shows the result of a calculation (solid curve) made with  $\varepsilon_0 = 14$  nm rad and  $\kappa = 0.015$  instead of the design values ( $\varepsilon_0 = 5$  nm rad and  $\kappa = 0.02$ ). An energy spread of  $1.13 \times 10^{-3}$  was also taken into account for this calculation.

The above selection of  $\varepsilon_0$  and  $\kappa$  was made on the basis of the measured spectrum (shown in Fig. 6). The combination of  $\varepsilon_0$  and  $\kappa$  greatly affects (a) the flux density (or brilliance) of each harmonic, (b) the bandwidth of each harmonic, and (c) the ratio of the flux density of an even harmonic to an odd one. Therefore,  $\varepsilon_0$  and  $\kappa$  may be well constrained inversely by observations concerning the above three items. Fig. 7 shows contour maps of (a) the flux density of the first harmonic ( $D_1$ ) of the radiation from the XU#MR0, (b) the bandwidth of the first harmonic ( $\Delta\omega/\omega_1$ ), and (c) the ratio of the second-harmonic flux density to

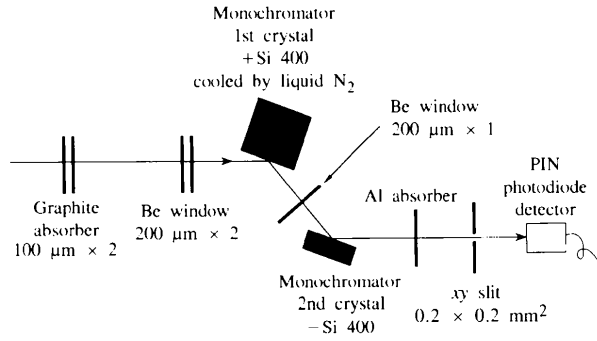


**Figure 5** Schematic diagram of the optics used for the spectrum measurement.

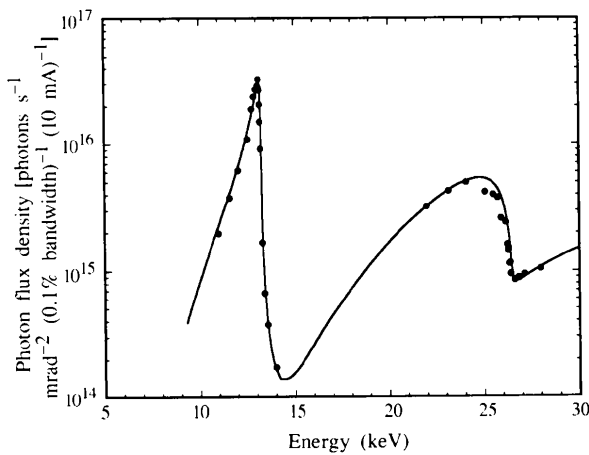


**Figure 6** Photon flux density of the radiation from the XU#MR0 with  $K = 1.09$  (the first harmonic energy is 13.1 keV) when the MR is operated at 10 GeV and 10 mA. The solid circles indicate the observed results (Fig. 5) and the solid curve indicates the result of a calculation made with a natural emittance ( $\varepsilon_0$ ) of 14 nm rad, an emittance coupling ( $\kappa$ ) of 0.015, and an energy spread of  $1.13 \times 10^{-3}$ .

the first ( $D_2/D_1$ ), which were calculated as functions of  $\varepsilon_0$  and  $\kappa$  using the same parameters as those used for the solid curve in Fig. 6. The observed results of  $D_1 = 3.3 \times 10^{16}$  photons  $s^{-1}$   $mrad^{-2}$  (0.1% bandwidth) $^{-1}$  and  $\Delta\omega/\omega_1 = 0.042$  (Fig. 6) are explained only by the combination of  $\varepsilon_0 = 14$  nm rad and  $\kappa = 0.015$ , as shown in Figs. 7(a) and 7(b). Since the number of unknowns to be obtained is two, the constraint conditions obtained from Figs. 7(a) and 7(b) are enough to determine the values of  $\varepsilon_0$  and  $\kappa$ . The condition obtained from Fig. 7(c) can be used for a redundancy check. Although the observed values which form the second

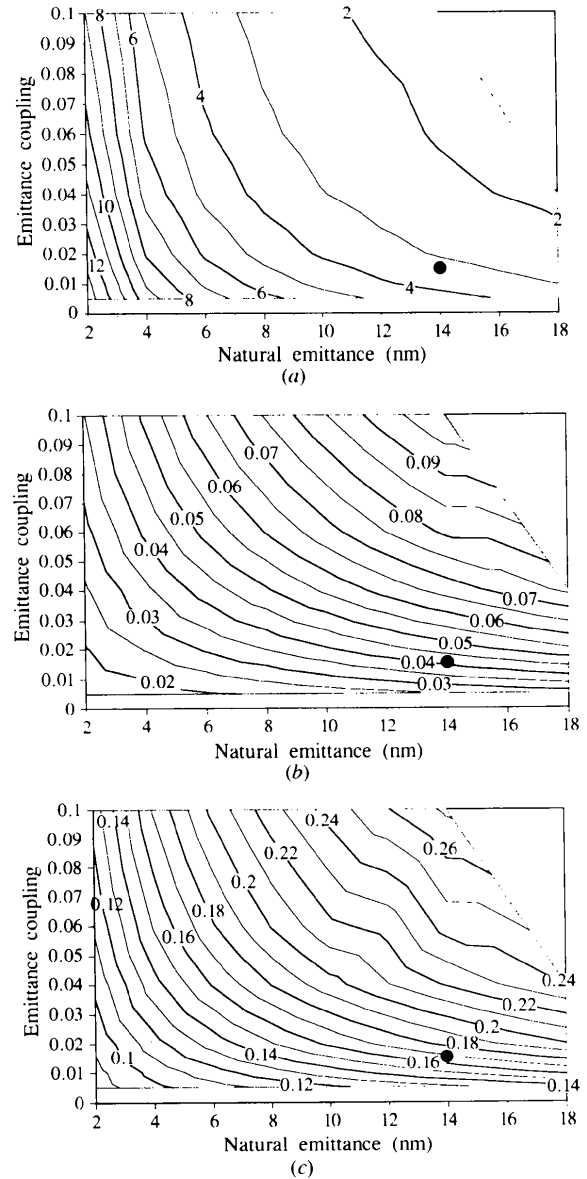


**Figure 7** Contour maps of (a) the flux density of the first harmonic ( $D_1$ ) of the radiation from the XU#MR0 [ $\times 10^{16}$  photons  $s^{-1}$   $mrad^{-2}$  (0.1% bandwidth) $^{-1}$  (10 mA) $^{-1}$ ], (b) the bandwidth of the first harmonic ( $\Delta\omega/\omega_1$ ), and (c) the ratio of the second-harmonic flux density to the first ( $D_2/D_1$ ), which are shown as functions of the natural emittance ( $\varepsilon_0$ ) and the emittance coupling ( $\kappa$ ). The solid circle indicates the point of the natural emittance,  $\varepsilon_0 = 14$  nm rad, and the emittance coupling,  $\kappa = 0.015$ .

harmonic are somewhat scattered, the ratio  $D_2/D_1 = 0.165$ , obtained from smoothing these data, is consistent with the result shown in Fig. 7(c). In this contour a combination of  $\varepsilon_0 = 14$  nm rad and  $\kappa = 0.015$  gives  $D_2/D_1 = 0.170$ . The agreement between observation and calculation strongly suggests that the electron-beam quality under the present operation of the MR should be expressed by  $\varepsilon_0 = 14$  nm rad and  $\kappa = 0.015$  as an effective emittance in the XU#MR0, including the effects from the above-mentioned ambient horizontal field. Further, the value of the vertical emittance ( $\varepsilon_y = 0.21$  nm rad), which was obtained on the basis of the observed value of  $\sigma_y = 6.6$   $\mu$ rad using  $\beta_y = 4.8$  m (design value), is very consistent with the above inference of the emittance.

The above condition of the emittance corresponds to a brilliance of  $6.9 \times 10^{17}$  photons  $s^{-1}$   $mm^{-2}$   $mrad^{-2}$  (0.1% bandwidth) $^{-1}$ , which does not amount to our target value of  $3.6 \times 10^{18}$  photons  $s^{-1}$   $mm^{-2}$   $mrad^{-2}$  (0.1% bandwidth) $^{-1}$  when  $K = 0.97$  with 10 GeV and 10 mA operation of the MR. However, our present attempt to convert the large accelerator to a light source having a very low emittance and high-quality beam was successful, in addition to the previous examples of the PEP at SLAC (Bienenstock, Brown, Wiedemann & Winick, 1989) and the PETRA at DESY (Balewski, Brefeld, Hahn, Pflüger & Rossmannith, 1995). We believe that the present success proves the basic potential for constructing coherent light sources along the lines of the present scheme.

The authors express their sincere thanks to the staff of the Tristan accelerator group for their collaboration in constructing the Tristan Super Light Facility. They would also like to express their thanks to Professor M. Ando for his help and critical discussion concerning the present study.

## References

- Balewski, K., Brefeld, W., Hahn, U., Pflüger, J. & Rossmannith, R. (1995). *Proc. 1995 Part. Accel. Conf.* pp. 275–277. Piscataway, NJ: Institute of Electrical and Electronic Engineers.
- Ban, S., Hirayama, H., Namito, Y., Tanaka, S., Nakashima, H., Nakane, Y. & Nariyama, N. (1994). *J. Nucl. Sci. Technol.* **31**, 163–168.
- Bienenstock, A., Brown, G., Wiedemann, H. & Winick, H. (1989). *Rev. Sci. Instrum.* **60**, 1393–1398.
- Kamada, S. (1997). In preparation. *Photon Factory Activity Report '95* (1997). Project. §A4–A5. Photon Factory, Tsukuba, Japan.
- Shiwaku, H. & Zhang, X. (1997). In preparation.
- Sugiyama, H., Zhang, X., Higashi, Y., Arakawa, E. & Ando, M. (1997). In preparation. *Tristan Super Light Facility; Conceptual Design Report 1992* (1993). Progress Report No. 92-1. KEK, Tsukuba, Japan.
- Yamamoto, S. (1995). *Photon Factory Activity Report '94*, pp. 5–8. Photon Factory, Tsukuba, Japan.
- Yamamoto, S., Shioya, T., Kitamura, H. & Tsuchiya, K. (1995). *Rev. Sci. Instrum.* **66**, 1996–1998.
- Yamamoto, S., Zhang, X., Kitamura, H., Shioya, T., Mochizuki, T., Sugiyama, H. & Ando, M. (1993). *J. Appl. Phys.* **74**, 500–503.